Fracture Energy of High-Strength Concrete in Compression

Dahl, Henrik; Brincker, Rune

Publication date:
1989

Document Version
Publisher's PDF, also known as Version of record

INSTITUTTET FOR BYGNINGSTEKNIK

INSTITUTE OF BUILDING TECHNOLOGY AND STRUCTURAL ENGINEERING

AALBORG UNIVERSITETSCENTER · AUC · AALBORG · DANMARK

FRACTURE AND DYNAMICS
PAPER NO. 11

HENRIK DAHL & RUNE BRINCKER

FRACTURE ENERGY OF HIGH-STRENGTH CONCRETE IN COMPRESSION

MAY 1989

ISSN 0902-7513 R8919

The FRACTURE AND DYNAMICS papers are issued for early dissemination of research results from the Structural Fracture and Dynamics Group at the Institute of Building Technology and Structural Engineering, University of Aalborg. These papers are generally submitted to scientific meetings, conferences or journals and should therefore not be widely distributed. Whenever possible reference should be given to the final publications (proceedings, journals, etc.) and not to the Fracture and Dynamics papers.

Fracture Energy of High-Strength Concrete in Compression

Henrik Dahl and Rune Brincker
University of Aalborg
Sohngaardsholmsvej 57, DK-9000 Aalborg
Denmark

ABSTRACT.

Compression tests are usually carried out in load control. This implies the termination of the test at the peak point of the load-displacement curve, while the fracture under these conditions becomes unstable at the descending branch of the load displacement relation. However, the descending branch is essential for understanding the fracture mechanisms of concrete in compression. In this paper a series of tests is reported, carried out for the purpose of studying the fracture mechanical properties of concrete in compression. Including the measurement and study of the descending branch, a new experimental method has been used to investigate the influence of boundary conditions, loading rate, size effects and the influence of the strength on the fracture energy of high-strength concrete over the range 70 MPa to 150 MPa, expressed in nominal values.

1. INTRODUCTION

As a result of concrete research in the last decades, it is today possible to design concrete with a compressive strength near 200 MPa. However the brittleness of high-strength concrete has made traditional methods of structural design uncertain, and therefore there is a need for development of experimental methods and systematic investigations in the area of brittleness of high strength concrete.

It is obvious to try to use the concepts of fracture mechanics on a this problem because fracture mechanics is a suitable theory for description of failure of brittle materials. The research of describing fracture of concrete by fracture mechanics has until now primarily been concentrated on fracture caused by tension [1]. Fracture of concrete in compression is more complicated, both in the theoretical and the experimental part, while the mode of the fracture is more complex.

Considering the fracture of concrete submitted to uniaxial compression from a fracture mechanical point of view two features are important; the fracture energy and the shape of the entire load-displacement curve. So far, only few researchers have

measured the descending branch of the load-displacement curve for concrete, [3], [5], even though the descending part of the curve is essential for the understanding and description of the fracture of high-strength concrete.

Professor S. P. Shah has developed a method making it possible to measure both the rising and the declining part of the load-displacement curve for a cylindric specimen submitted to uniaxial compression [3]. In this method the test is controlled by using the longitudinal deformation as feedback at the ascending branch and the circumferential deformation as feedback signal at the descending branch of the stress-strain relation.

In this test series the basic idea of Shah was used, i.e. the circumferential deformation was used as feedback signal. However, it proved to be convenient to modify the method so that the same control set-up could be used both before and during the different stages of the test.

2. SPECIMENS

The test series were performed on cylindrical specimens made of three different high-strength concretes. The nominal strengths of the concretes used were: 70 MPa, 110 MPa and 150 MPa.

The three types of concrete were all having identitical content of stone and sand. The mix proportions are shown in table 1.

INGREDIENTS Type	MIX 1 $\frac{kg}{m^3}$	MIX 2 $\frac{kg}{m^3}$	MIX 3 $\frac{kg}{m^3}$
CRUSHED AGGREGATE:			
"Dura-split" 5 - 8 mm	360	360	360
"Dura-split" 2 - 5 mm	721	721	721
"Quarts sand 1 - 2 mm	289	289	289
"Quarts sand 0.25 - 1 mm	392	392	392
PORTLAND CEMENT (low alkali)	567	657	502
SILICA FUME	0	0	169
DISPERGENT AGENT (powder)	0	16.4	17.0
WATER	170	131	102

Table 1. Mix proportions for the three types of concrete.

The specimens were cast under vibration and cured for 1 day at 20^0 C in closed form and then 2 days in water at 80^0 C.

After curing the specimens 2 days at 80^0 C the strength was almost fully developed, and influence on test results from the time difference between the tests could therefore be neglected.

Because of the limited capacity of the testing machine used in these test series - Schenck Hydropuls PSB 25 with a capacity of 250 kN - the sizes of the specimens had to be relatively small. Three different sizes of cylinders were used:

Type 1: 34 mm diameter and 70 mm height.
Type 2: 45 mm diameter and 90 mm height.
Type 3: 57 mm diameter and 120 mm height.

3. TEST ARRANGEMENT

A test arrangement for measurement of the total stress-strain relation in compression must by designed giving priority to system stiffness. If not, accumulation of elastic energy could lead to fatal fracture when the energy is released on the descending branch of the load-displacement relation.

To ensure a uniform stress distribution at the ends of the specimen, boundary layers were applied between the specimen and the steel parts, and a spherical bearing was applied between the specimen and the upper fixed compression head of the testing machine. Application of bearings and boundary layers implies a reduction of the system stiffness, but it was found necessary in this way to compromise between the demand for stiffness and the demand for uniform stress distribution.

A lack of stiffness in the mechanical system can be compensated by choosing a high response servo control system, i.e. a system with fast responses of the servo controller, servovalve, actuator etc. To meet these requirements a high performance testing machine, the Schenck Hydropuls PSB 25, was used for the tests.

The tests were controlled by a feedback signal that included contributions from both the piston displacement and the longitudinal and circumferential deformation of the specimen. The feedback signal δ was created by analog addition of the corresponding electrical signals :

$$\delta = \delta_c + \alpha\delta_l + \beta\delta_p \tag{1}$$

where δ_c, δ_l and δ_p are the circumferential deformation, the longitudinal deformation and the piston displacement respectively. The weight factors α and β were taken empirically as $\alpha = 1.60$ and $\beta = 64.0$.

The main idea in using this combined signal as feedback signal in a closed loop servo control is that the different terms in eq. (1) each plays a dominant role in the different stages of the test.

The piston displacement contribution allows for an easy start-up procedure where the piston is moved by traditional displacement control, since the other contributions are constant as long as the load is zero.

At the ascending branch of the stress-strain relation, the longitudinal displacement is dominant, and the test is controlled as in traditional strain control. This changes after the peak point where the longitudinal strain is approximately constant or even decreasing during the fracture process. At the descending branch an intense development of uniformly distributed cracks causes a significant increase in circumferential strain response, see fig. 2.a, and the contribution to the feedback from the circumferential deformation becomes dominant. The control system is shown in fig. 1.

The longitudinal deformation was determined as the mean value of the signals from two LVDTs measuring the distance between the lower compression head and the spherical bearing. The LVDTs had a 20 mm base and the sensitivity was conditioned to $C_l = 0.40$ mm/Volt.

The circumferential deformation was measured as described by Shah [3], by a string wrapped around the centre of the cylinder, which was connected to a LVDT transducer. The LVDT had a 10 mm base and the sensitivity was $C_c = 1.00$ mm/Volt.

The piston displacement was measured by the built-in LVDT having an 80 mm base and a sensitivity of $C_p = 8.0$ mm/Volt.

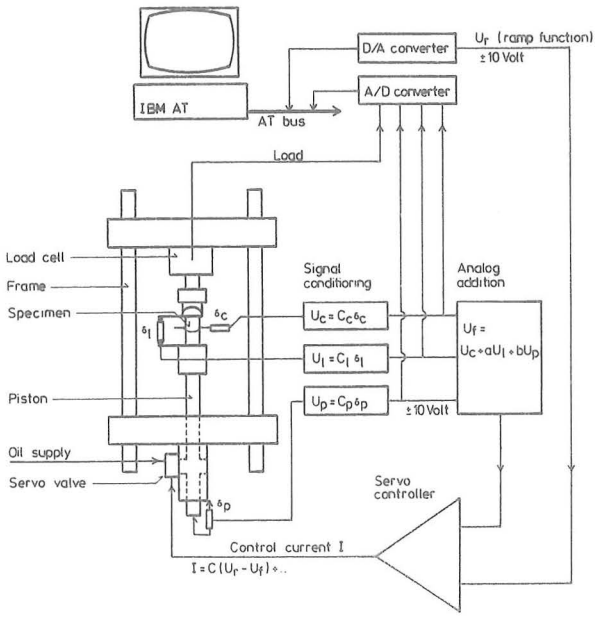

Figure 1. The entire test and control arrangement.

The reference signal in the servo control loop was continuously transmitted from a Personal Computer by a digital to analog converter, according to the loading rate chosen. At the same time the time t, the load F and the displacements δ_l and δ_c were recorded at the same computer using an analog to digital converter, see fig 2.

4. DATA REPRESENTATION

In the following sections results are given in terms of stress-strain relationships and fracture energies.

All stress-strain relationships shown are determined directly from the raw data, i.e. no corrections are made for excess deformation in boundary layers, friction between piano string and specimen, etc. The only effect corrected for is elastic deformation in steel parts found by measuring the load displacement relationship with no specimen in the test machine.

The uniform compression stress σ was determined as the compression load F divided by the nominal cross sectional area A of the specimen. The longitudinal strain ϵ_l was determined as the measured longitudinal deformation δ_l divided by the nominal specimen deptht l, and the circumferential strain ϵ_c was determined as the measured circumferential deformation δ_c divided by the nominal circumference of the specimen $2\pi r$, r being the nominal radius of the specimen.

Fig. 4.a shows a typical stress-strain relation. The change in strain response from the ascending to the descending branch is remarkable. At the ascending branch the response is approximately linear in both longitudinal and circumferential strain. The circumferential strain response, however, is absent in fig. 2.a at this stage of the test because of low sensitivity (to allow for high fracture strains) and friction between piano string and specimen. At the descending branch the longitudinal strain is constant or even decreasing (snap back) while the circumferential strain shows a remarkable increase in response. At the descending branch the ratio between circumferential strain and longitudinal strain was typical 20 to 30 implying a volume strain (much) greater than zero.

Unbiased values for the fracture energy G for the different tests could not be estimated, because, for some practical reasons, all tests were terminated before total fracture, i.e. there was still some load-carrying capacity left in the specimen. Furthermore, the different specimens showed a rather different behaviour at the descending branch. Some stress-strain relationships showed a very fast decrease in load-carrying capacity (thin and short tail) and others showed a much more slow decrease in load carrying capacity (long thick tail). Since the stress-strain curves did not share a common form at the descending branch, no corrections could be made for the energy in the missing tail.

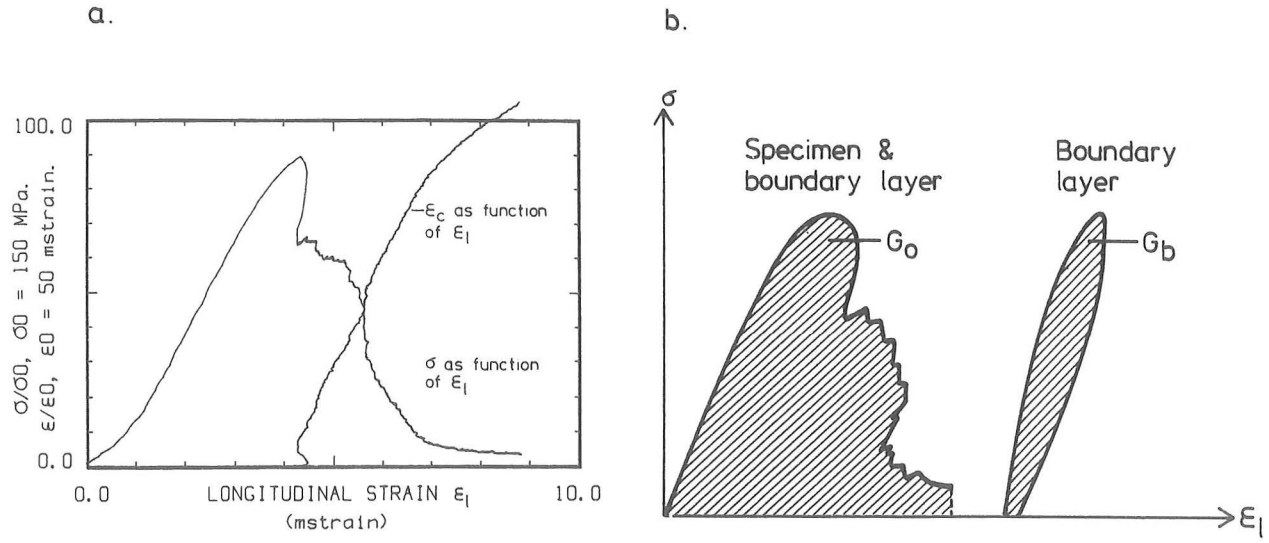

Figure 2.a: Typical stress-strain relation obtained by test. 2.b: Determination of the fracture energy G_f

If a test for some reason (typical reason was instability in control system) was terminated at a load that was greater than one third of the ultimate load, then the test was considered unsuccessful, and the fracture energy was not calculated. On the other hand, if the test was terminated at a load that was smaller than one third of the ultimate load, then the test was considered successful, and the fracture energy G_f was determined by:

$$G_f = G_0 - G_b \tag{2}$$

where G_0 was calculated as the area under the truncated stress-strain curve and G_b is the energy dissipated in the boundary layer. The energy G_b dissipated in the boundary layer could not be estimated directly, but was determined by separate tests using a steel cylinder instead of the concrete specimen. See fig. 2.b. It is believed that the energy dissipated in the boundary layer was underestimated when determined in this way, because friction and slip is greater between concrete and layer than between steel and layer. However, no method of correcting this error was found.

5. BOUNDARY CONDITIONS

To interpret the test results, it is important to know the influence of boundary conditions on the slope of the load-displacement curve and on the value of the fracture energy, [5]. To investigate this problem, six different boundary conditions were tested on ø45 cylinders (type 2), made of a concrete with a nominal strength of 110 MPa (mix 2). All cylinders used in this investigation were from the same batch. As boundary layers the following materials were used: nothing (dry friction between specimen surface and steel parts), 0.5 mm teflon, 0.5 mm rubber, 0.8 mm soft cardboard, 0.1 mm paper, and two steel plates glued to the ends of the specimen.

In each series, except for the paper boundary layer, 7 tests were carried out, but not all were successful. For the paper boundary layer only 4 tests were carried out.

The results are shown in fig. 3. The influence from boundary conditions are significant. The boundary conditions dry friction, glued steel plates and paper layers do not show great difference, but the remaining boundary conditions teflon layers, cardboard layers and rubber layers both show a significant mutual difference and significant different behaviour compared to the first mentioned boundary conditions.

Furthermore, it is worth noticing that the tails of the stress-strain relationships are much longer and thicker when using rubber or teflon than for the other boundary conditions. This is believed to be due to the special friction conditions when using these layers. Teflon has a very low friction against smooth steel, especially under high pressure. Rubber in a thin layer will under high pressure develop "negative friction" on the specimen. This suggests - and is confirmed by observations during the tests - that for the rubber and teflon boundary layers, the mode of fracture is different from the usual hour-glass mode of fracture. The fracture when using boundary layers with very low friction will be more homogeneous, i.e. the cracks will tend to arrange in a uniformly distributed pattern of vertical cracks.

No adjustments due to boundary conditions were made on tests with steel plates glued to the specimens, because virtually no energy will dissipate in the joint compared to the energy dissipated in the concrete cylinder, as long as no fracture occurs in the bonded joint. However, it is not possible to know if the bonded joint between steel and specimen could yield or crack during the tests. This uncertainty is due to the complicated interaction between concrete fracture and joint fracture. Even if the glued steel plates seem to represent a well-defined boundary condition, the alternative was not considered for the reasons mentioned above.

The reduced fracture energies for the different boundary conditions determined as the average value for each series are listed in table 2. The energies dissipated in boundary layers were about 20-30 Nm for both rubber and cardboard and about 2-6 Nm for the other layers except energies dissipated in the bonded joints between specimens and steel plates which were assumed to be zero.

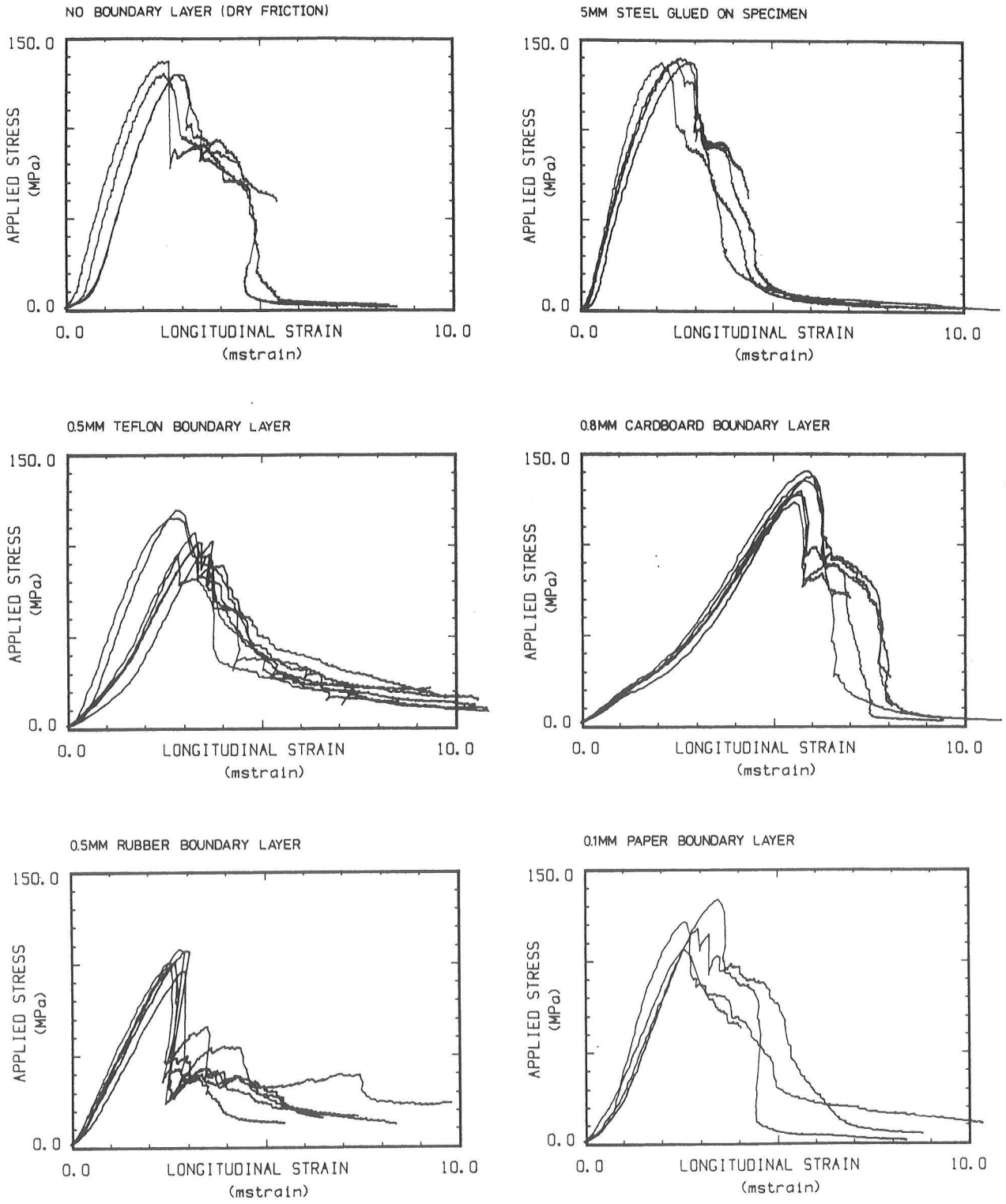

Figure 3. Stress- strain relationships measured on the same type of specimens but using different kinds of boundary layers.

No boundary layer (dry friction)	58.0
0.5 mm teflon layer	56.2
0.5 mm rubber layer	22.0
0.8 mm soft cardboard	55.8
0.1 mm paper layer	51.1
Glued steel plates	56.4

Table 2. The fracture energy in Nm for the different boundary conditions.

It is seen from the result given in table 2, that there is no significant difference in fracture energy, except for the tests with rubber boundary layer which seem to halve the measured fracture energy.

The paper boundary layer was chosen for further experiments. The reasons for this choice were primarily the relatively small energy dissipated in the layer, a well defined friction, and good experience with the layer in order to perform tests with a high success rate. For example it proved difficult to use dry friction (no boundary layer) because this boundary condition had a high rate of unsuccessful tests (tests became unstable at the descending part of the stress-strain relation).

6. LOADING RATE

The loading rate was expected to have influence on the value of the fracture energy and on the shape of the stress-strain curve. It is well known that the strength increases with loading rate [2].

Nine different load rates were applied to ø45 mm cylinders (type 2) and measurements were made on 70 MPa strength class (mix 1) where the measured strength was 88 MPa.

Four tests were carried out at each loading rate, and only a few were unsuccessful.

The loading rates on the ascending branch of the stress-strain curve varied from 0.31 MPa/sec. to 40.24 MPa/sec., the ratio between the highest and lowest loading rate being about 130.

When the loading rate was 40.24 MPa/sec. the peak point was reached after about 3 seconds, and the whole test ended after about 15 seconds. The loading rate for the boundary condition tests and the tests reported in the following sections were 1.26 MPa/sec.

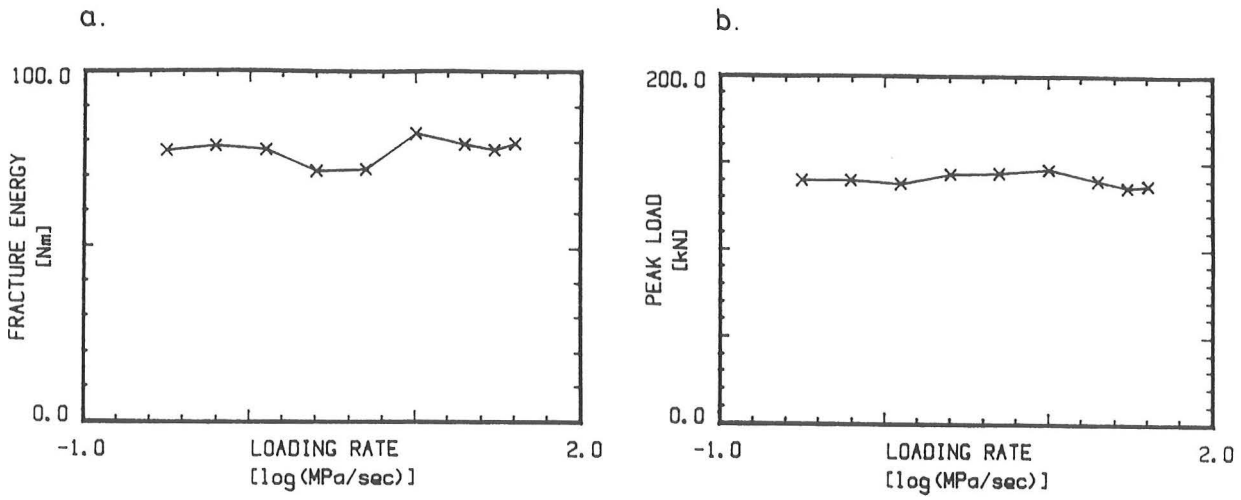

Figure 4.a: The fracture energy for different loading rates. 4.b: The peak loads for different loading rates.

In contradiction to what was expected the fracture energy was relatively constant over the range of loading rates applied, see fig. 4.a. The peak load was also constant with respect to different loading rates, see fig. 4.b, which indicates that the shape of the load-displacement curve does not depend on the loading rate.

7. SIZE EFFECTS

In tension, the fracture energy per cracked area (energy release rate) is usually assumed to be a material constant, and standard tests have been developed for an easy study of this assumption and the establishment of relationships between fracture energy and concrete mix, Hillerborg [5]. In compression, however, it is not possible to investigate this assumption directly, because the cracked area is not well defined since the cracks spread over most of the specimen.

If the crack pattern is uniformly distributed over the whole volume, it is obvious to assume that the fracture energy per volume is a material constant. On the other hand, if the fracture is concentrated in a limited zone, what could be expected if the depth of the specimens was increased, it would be plausible to assume the energy per cross-sectional area as a material constant. For a usual compression test, and for the tests carried out in this test programme, the mode of failure can be classified as something falling between these two cases. It was therefore not expected that any of the two simple models could explain the test results.

To investigate the size dependence tests were performed on three different cylinder sizes: ø34 mm, ø45 mm and ø57 mm. All cylinders were made from 70 MPa

concrete (mix 1). The measured average compressive strength was 78 MPa for ø34 mm, 92 MPa for ø45 mm and 84 MPa for ø57 mm. Ten tests were performed for each strength.

The fracture energy per cross sectional area increased with specimen size, see fig. 5.a, but the increase in energy is relatively small; about 30 % increase from the smallest to the largest specimen.

This result, however, is in contrast to results from fracture energy measurements on concrete in tension. Hillerborg reports, that for the three point bending test [4] the fracture energy release rate decreases by about 20 %, when the cross-sectional area of the specimen doubles. For the compression test however the fracture energy per cross-sectional area increases about 20 % when the area doubles.

The fracture energy per volume as a function of the area was not constant either. As expected the energy per volume decreases with the cross sectional area, see fig. 5.b.

This indicates, as earlier mentioned, the existence of a fracture zone, i.e. the volume of the part of the body that is in fracture, becomes a relatively smaller part of the body as the size of body increases.

It can therefore be concluded that the fracture energy dissipates in a combined form of surface work (fracture mechanical point of view) and volume work (plasticity). However, one would expect the fracture energy per cross-sectional area to become independent of specimen size, if the specimen was large enough. This size effect is indicated in fig. 5.a, where the results show a decreasing slope for increasing size of specimen.

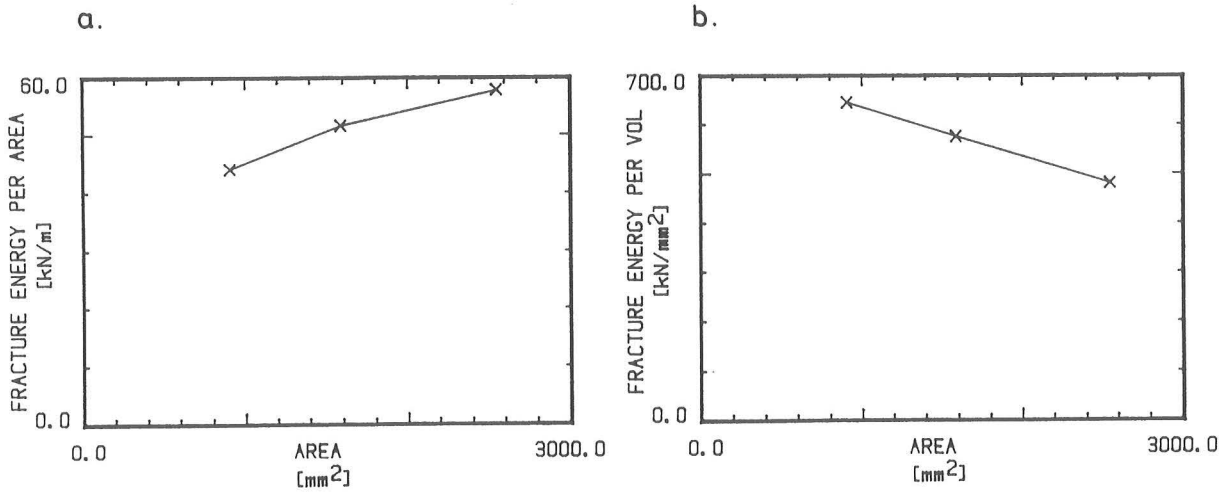

Figure 5.a: The fracture energy per cross-sectional area as a function of the cross-sectional area of the cylinder. 5.b: The fracture energy per volume as a function of the cross-sectional area of the cylinder.

8. INFLUENCE OF STRENGTH ON FRACTURE ENERGY

To investigate the influence of the compression strength of the concrete upon the fracture energy, tests were performed on specimens made from concretes with different strengths. Three different strengths of concrete were used: 70 MPa, 110 MPa and 150 MPa (mix 1,2 and 3). Because of the limited capacity of the test machine (250 kN), the ø35 mm cylinders (type 1) were used. The measured strengths were 86 MPa, 127 MPa and 155 MPa, respectively.

Ten cylinders were tested successfully for each type of concrete. The dependence of the strength on the fracture energy is shown in fig. 6.

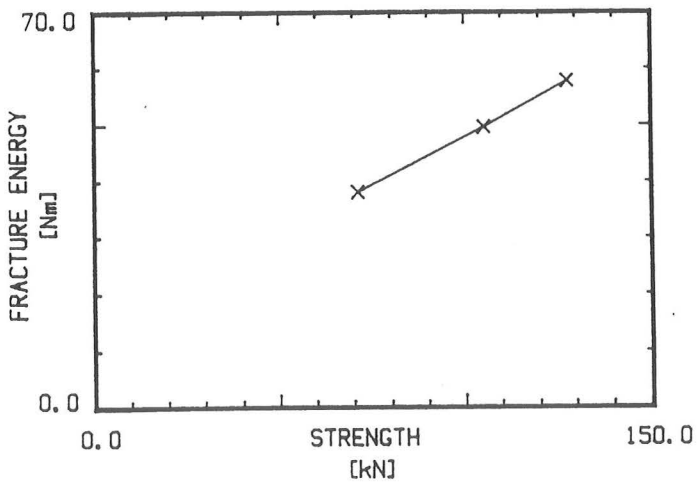

Figure 6. The fracture energy as a function of the compression strength.

The relation between fracture energy and cylinder compression strength is seen to be approximately linear, but a straight line estimation would clearly yield a linear expression with a constant greater than zero, i.e. the straight line estimation does not go through the origin. This shows that the linearity is not valid for lower strength classes of concrete, since the relation between strength and fracture energy must go through the origin. Furthermore it indicates that the brittleness of normal-strength concrete is more strength sensitive than the brittleness of high-strength concrete.

9. CONCLUSIONS

From the series of tests made on ø34 mm, ø45 mm and ø57 mm cylinders produced in three different strength classes: 70 MPa, 110 MPa and 150 MPa, the following conclusions can be drawn:

1. The test and control system developed for the tests proved to be efficient and easy to use. The principle of measuring the circumferential deformation by a string wrapped around the centre of the cylinder proved reliable and was capable of controlling the test during all stages of the test when used as one of the components of a feedback signal also consisting of signals from the longitudinal deformation and the piston displacement.

2. Ideal boundary conditions were difficult to obtain, because of energy dissipated in the boundary layers and because of differences in friction properties causing unacceptable variation in shear stresses on the end surfaces of the specimens. The load-displacement relation was strongly dependent upon the type of boundary layer.

3. The loading rate had no significant influence on neither the peak forces nor the value of the fracture energy.

4. The size effect was significant both on the fracture energy per cross-sectional area and on the fracture energy per volume. The fracture energy per cross-sectional area increased and the fracture energy per volume decreased with the size of the specimens. This may be taken as an indication that the fracture zone is smaller than its "natural size", and that size effects on the fracture energy per volume should be expected to increase and size effects on fracture energy per cross-sectional area should be expected to decrease if larger specimens were used. The test results also support these assumptions.

5. The fracture energy did not increase in the same proportion as the strength, clearly indicating that the brittleness increases with strength - an effect well known from tension tests. Furthermore, the test results indicate a stronger dependence of strength on brittleness for normal-strength concrete than for high-strength concrete.

ACKNOWLEDGEMENTS

We are grateful to Mr. H.H. Bache and T. Bach, Aalborg Portland for practical advice and assistance and to Dr. H. Krenchel, Department of Structural Engineering, DTH for stimulating discussions in the initial phase of the test programme.

Financial support from the Danish Technical Research Council is gratefully acknowledged.

REFERENCES

[1] Hillerborg, A.: A Model for Fracture Analysis. Report TVBM-3005, 1978, Division of Building Materials, Lund Institute of Technology, Sweden.

[2] Rüsch, H.: Researches Toward a General Flexural Theory for Structural Concrete. Journal of A.C.I. Proc., Vol. 57, No. 1, 1960.

[3] Shah, S. P.; Godoz, U.; Ansari, F: An Experimental Technique for Obtaining Complete Stress-Strain Curves for High Strength Concrete. ASTM Cement, Concrete and Aggregates, vol. 3, No. 1, 1981.

[4] Hillerborg, A.: Results of Three Comparative Test Series for Determining the Fracture Energy G_F of Concrete. Materiaux et Constructions, vol. 18, No. 107, 1985.

[5] Kotsovos, M. D.: Effect of Testing Techniques On the Post-Ultimate Behaviour of Concrete in Compression. Materiaux et Constructions, vol. 16, No. 91, 1983.

[6] Hillerborg, A.: The Theoretical Basis of a Method to Determine the Fracture Energy G_f of Concrete. Materiaux et Constructions, vol. 18, No. 106, 1985.

FRACTURE AND DYNAMICS PAPERS

PAPER NO. 1: J. D. Sørensen & Rune Brincker: *Simulation of Stochastic Loads for Fatigue Experiments.* ISSN 0902-7513 R8717.

PAPER NO. 2: R. Brincker & J. D. Sørensen: *High-Speed Stochastic Fatigue Testing.* ISSN 0902-7513 R8809.

PAPER NO. 3: J. D. Sørensen: *PSSGP: Program for Simulation of Stationary Gaussian Processes.* ISSN 0902-7513 R8810.

PAPER NO. 4: Jakob Laigaard Jensen: *Dynamic Analysis of a Monopile Model.* ISSN 0902-7513 R8824.

PAPER NO. 5: Rune Brincker & Henrik Dahl: *On the Fictitious Crack Model of Concrete Fracture.* ISSN 0902-7513 R8830.

PAPER NO. 6: Lars Pilegaard Hansen: *Udmattelsesforsøg med St. 50-2, serie 1 - 2 - 3 - 4.* ISSN 0902-7513 R8813.

PAPER NO. 7: Lise Gansted: *Fatigue of Steel: State-of-the-Art Report.* ISSN 0902-7513 R8826.

PAPER NO. 8: P. H. Kirkegaard, I. Enevoldsen, J. D. Sørensen, R. Brincker: *Reliability Analysis of a Mono-Tower Platform.* ISSN 0902-7513 R8839.

PAPER NO. 9: P. H. Kirkegaard, J. D. Sørensen, R. Brincker: *Fatigue Analysis of a Mono-Tower Platform.* ISSN 0902-7513 R8840.

PAPER NO. 10: Jakob Laigaard Jensen: *System Identification1: ARMA Models.* ISSN 0902-7513 R8908.

PAPER NO. 11: Henrik Dahl & Rune Brincker: *Fracture Energy of High-Strength Concrete in Compression.* ISSN 0902-7513 R8919.

PAPER NO. 12: Lise Gansted, Rune Brincker & Lars Pilegaard Hansen: *Numerical Cumulative Damage: The FM-Model.* ISSN 0902-7513 R8920.

Institute of Building Technology and Structural Engineering
The University of Aalborg, Sohngaardsholmsvej 57, DK 9000 Aalborg
Telephone: Int.+45 8 14 23 33 Telefax: Int.+45 8 14 82 43